Design Principles and Dynamic Front End Reconfiguration for Low Noise EEG Acquisition with Finger Based Dry Electrodes

Viswam Nathan, *IEEE Student Member*, and Roozbeh Jafari, *IEEE Senior Member*

***Abstract*—Dry electrodes are a convenient alternative to wet electrodes for electroencephalography (EEG) acquisition systems. Dry electrodes are subject to a higher amount of noise at the electrode scalp interface and these effects can be worsened due to non-ideal design or improper placement on the head. In this work, we investigate a popular dry electrode design based on a number of resistive 'finger' shaped contacts. We conduct experiments comparing designs with varying numbers of fingers using two impedance measurement methods and show that sparser arrangements of fingers are more robust to varying use cases and are more effective at penetrating through hair on the scalp. We then show that these impedance measurement metrics could be used to sort individual fingers within one electrode according to quality of electrical contact. We show that the signals from individual fingers can differ from each other significantly due to differing local effects of impedance and noise, and demonstrate through experimental results that dynamically selecting only a subset of fingers with good contact impedance can improve the overall signal-to-noise ratio of the EEG signal from that electrode.**

***Index Terms*—Dry contact EEG, Skin electrode noise.**

I. Introduction

BRAIN computer interface (BCI) provides an excellent non-muscular avenue for a user to interface with an external device. A good BCI infers the user's intentions by interpreting the measured brain signals, perhaps elicited as a result of a specifically designed paradigm, and performs the required action or actuation. This method of communication and control would be a very valuable asset in improving the quality of life of otherwise physically disabled individuals such as patients diagnosed with amyotrophic lateral sclerosis (ALS) or other paralyzing conditions [1].

A common technique on which BCIs are based is the capturing of electroencephalographic (EEG) activity through the use of conducting electrodes placed on the scalp. To meet the requirements of a wearable BCI system for long term monitoring, the electrodes need to be designed such that they are convenient to use, consistently maintain sufficient quality of contact and are less susceptible to noise sources that would interfere with clean EEG signal acquisition.

Manuscript submitted for review on 01/15/15. This work was supported in part by the Semiconductor Research Corporation, task # 1836.103 through the Texas Analog Center of Excellence (TxACE)

Viswam Nathan and Roozbeh Jafari are with the Center for Remote Health-care Technologies and Systems at Texas A&M University, College Station, Texas, 77843, USA. (e-mails: {viswamnathan,rjafari}@tamu.edu)

Wet or gel-based electrodes still represent the standard for medical grade EEG equipment [2]. Several noise sources associated with EEG acquisition have been linked to high impedance contact and so the gel solution in wet electrodes helps to create a suitably low impedance interface with the scalp. The signal-to-noise ratio (SNR) is consequently excellent for wet electrodes. However most wet electrode based systems require long preparation times and regular reapplication of the gel is needed to prevent the contact interface from drying out after long time periods. Wet electrode systems also sometimes require scalp abrasion to improve contact, causing scalp irritation and posing an infection risk. For all these reasons wet electrodes are not typically considered a convenient, viable option for a wearable system capable of long term EEG monitoring and BCI use [3].

Dry contact electrodes on the other hand, are generally easy for the user to put on autonomously, require no special preparation and are suitable for continuous long term use without significant degradation of contact quality. However the obvious drawback compared to wet electrodes is the relatively significant increase in noise pickup.

A typical design for dry electrodes is a number of conductive fingers, arranged in a circle, that are meant to penetrate through the hair and make a resistive contact with the scalp [4-6]. Examples of such electrodes are shown in Figure 1. The plurality of fingers is primarily for stability and redundancy of contact. Ultimately all the fingers are shorted together to give one channel of EEG per electrode.

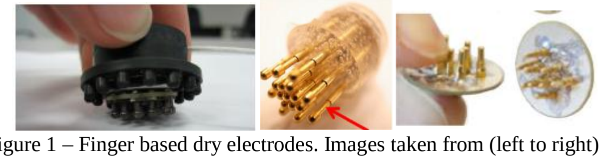

Figure 1 – Finger based dry electrodes. Images taken from (left to right) [4-6]

To our knowledge, there has been no previous systematic study looking into the trade-offs involved in choosing the number of fingers in a given design. The first part of the study described in this article provides experimental results that shed light on which designs are more robust and effective, and in doing so also presents a methodology for comparing different designs of dry electrodes in general.

There has also been no previous study analyzing the signals from each individual finger and the dynamics of the mixed signal obtained when all the fingers are shorted together. It is reasonable to expect that the different fingers on one electrode have different contact qualities for reasons such as skewed placement of the electrode or the interference of hair or sweat causing local effects on only some fingers. One question that follows is whether these local noise effects on a subset of fingers can adversely affect the overall EEG signal acquired from the combination of all fingers. If this is indeed the case, a natural follow-up question would be whether excluding these 'bad contact' fingers from the circuit improves the SNR of EEG acquisition. In order to investigate this we built two designs of electrodes for this second part of the study: an Individual Finger Channel (IFC) electrode to study and compare the signals picked up by individual fingers; and a Multiplexer (MUX) electrode that can disconnect any given finger from the overall signal path.

This article aims to grant a deeper insight into the electrode skin interface noise for dry electrodes, provide guidance for the improvement of existing finger-based electrode designs and propose a novel extension to the design that enables dynamic reconfiguration of the fingers to continually strive for better contact under varying scalp conditions and use cases.

II. Related Works

The finger based dry electrode design itself has been presented in a few previous studies. In fact, the part used for the fingers and the active electrode design for this work were borrowed from [6]. In most of these works, a given dry electrode design is either independently measured for noise performance or is compared to a wet electrode in order to validate its performance. By contrast, in this work we compare different versions of finger-based dry electrodes to each other and attempt to draw some conclusions to aid design decisions. This approach was initially presented in our previous work [7] and is discussed further here. In addition, the analysis of individual finger contacts and the idea of selecting a subset of fingers have not been explored before by others; however the impedance measurement technique [8] and the assumptions about the associated noise at the electrode-skin interface [2, 9] are gleaned from previous studies. This idea of finger selection was also previously explored by us in [10] and it is supported and discussed more comprehensively in this article.

III. Background

There are many sources of noise that affect EEG acquisition: motion artifacts, 50/60Hz interference, capacitive interference, the half-cell effect and others [2, 9]. In this study, the electrodes are designed to be buffered and shielded to mitigate external interference, and motion artifacts are beyond the scope of this work. We are however concerned with noise sources that affect the electrode scalp interface and it has been shown that the effect of these noise sources is exacerbated by high impedance contact. The half-cell effect, for example, happens when the metal of the electrode comes into contact with an electrolyte such as salt and sweat on the skin, causing an exchange of ions and the development of a potential difference directly proportional to the impedance of contact. Even for external interference, lower impedances of electrodes usually means better impedance matching and hence better rejection of common mode interferences such as 50/60Hz noise. Therefore, scalp electrode impedance can be used to compare the effectiveness of different electrodes as well as different fingers on one electrode. Figure 2 shows the details of the impedances involved in the contact with the scalp [2, 5].

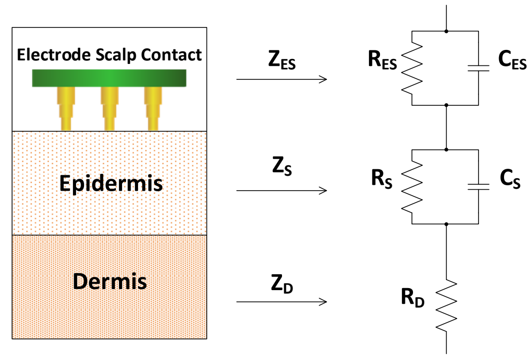

Figure 2 - Electrode skin circuit model (Image taken from [7])

Z_{ES} denotes the electrode scalp impedance due to the contact of the fingers. Z_S denotes the impedance of the epidermis layer of the skin, whereas Z_D denotes the impedance of the inner dermis layer. The overall impedance faced by the electrode is given by the series combination:

$$Z_{electrode} = Z_{ES} + Z_S + Z_D \quad (1)$$

The type of finger used and the overall size of the electrodes remains the same in the electrodes studied in this work; hence we hypothesize that any major differences in the performances across electrode types will be due to the effect of high resistance contact with hair and electrode designs that avoid hair consistently, thus minimizing Z_{ES}, will perform better.

Figure 3 shows the overall circuit model when two differential electrodes are used to measure EEG on the scalp.

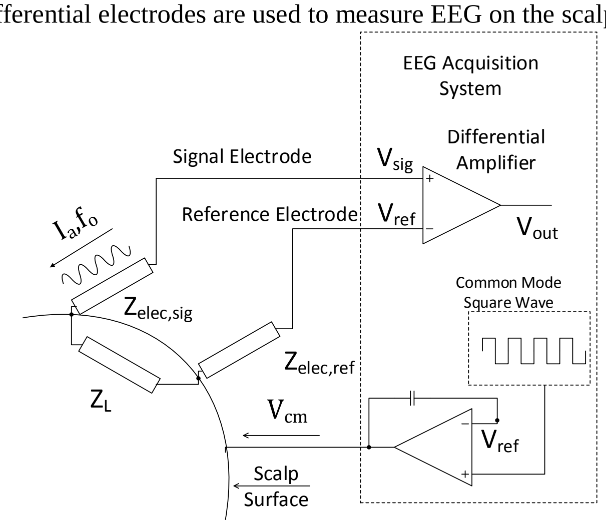

Figure 3 - Scalp impedance circuit with signal and reference electrodes (Image taken from [7])

The positive or 'signal' electrode measures V_{sig} with respect to ground, whereas the negative or 'reference' electrode measures V_{ref} with respect to ground. If $Z_{overall}$ denotes the overall impedance between the two electrodes, we have:

$$Z_{overall} = Z_{elec,sig} + Z_L + Z_{elec,ref} \quad (2)$$

The first term $Z_{elec,sig}$ gives the impedance faced by the signal electrode, which is the same as $Z_{electrode}$ in (1). Similarly, $Z_{elec,ref}$ refers to the impedance faced by the reference electrode. In this work, the layout of the dry electrode used as the signal electrode is varied, but the reference electrode is always a wet adhesive patch. Consequently, in the model for the reference electrode, instead of the finger impedance Z_{ES} we have the impedance of the gel, Z_G. So we can re-write (2) as:

$$Z_{overall} = (Z_{ES} + Z_S + Z_D) + Z_L + (Z_G + Z_S + Z_D) \quad (3)$$

The additional term Z_L represents the impedance of the length of scalp between the two electrodes. Using an adhesive electrode for the reference is evidently not feasible for a wearable EEG system, however for the purposes of comparing different types of dry electrodes we did not want to introduce the uncertainty of using a dry electrode for the reference as well. We assume all impedances except Z_{ES} described in (3) remain constant during all experiments. For the second part of the study involving individual finger analysis and finger selection, the model still applies but here Z_{ES} represents a single finger or a subset of selected fingers.

IV. Hardware Description

A. EEG Acquisition Board

We used a custom platform that uses the TI ADS1299 analog front end for 8-channel EEG acquisition, an MSP430 microcontroller and Bluetooth for wireless data transmission. This platform has been verified for BCI tasks and more details can be found in our previous works [11-13].

B. Traditional Finger Based Dry Electrodes

In this section, we provide brief physical descriptions of the various electrodes used for the study looking into the effects of varying the number of fingers and their arrangement in the traditional finger based dry electrode design.

Figure 4(a-e) shows the five different configurations, with the number of fingers ranging from 8 to 20, designed and evaluated in this work. For all the electrode designs, the distance from the center of the PCB to the outermost ring of fingers is 0.72cm, so the span of scalp coverage is the same for all electrodes. We used gold plated, spring loaded fingers of height 0.45cm and diameter 0.11cm at the point of contact.

We also included the g.SAHARA dry electrode by g.tec [14] (Figure 4(f)) in all our experiments just to ensure that the results from our custom electrodes are comparable to that of a commercially available one. This electrode also has an outer ring of 8 fingers similar to the 'Default 8' (Figure 4(e)).

C. Individual Finger Channel (IFC) Electrode

For the second part of the study looking into the local noise effects for each individual finger contact of the electrode, we built an electrode that isolated the signals from each finger into separate channels. The electrode built for this purpose (Figure 5) has an overall PCB height of 3.76cm, and consists of 8 fingers arranged and spaced in the exact same 'Default 8' configuration described earlier. However, the difference with this design is that the signal from each finger is immediately buffered before being sent through the cables into separate channels of the ADC on the EEG board. Figures 7(a) and 7(b) illustrate the difference between a traditional finger-based electrode and this custom IFC electrode respectively.

Figure 5 – IFC electrode front and back (Image taken from [10])

Our hypothesis is that the overall signal from the traditional electrode in Figure 7(a) could be improved by rejecting the individual signals from one or more fingers in the circuit if they are picking up too much noise. Using an estimate of the impedance on each finger, we can generate the mixed signal that would be obtained from any combination of fingers on the IFC electrode. This can be used to test the hypothesis, and the methods to do so are described in detail in Section V-C. It must be stressed that this electrode is not meant to be a practical replacement for existing EEG electrodes, and is merely intended for exploratory analysis looking into the difference between individual fingers' signals on one electrode.

D. Multiplexer (MUX) Electrode

In order to validate the analysis from the IFC electrode, we also designed a MUX electrode that can actually switch between using any combination of 8 fingers using an 8:1 analog MUX. Figure 6 and Figure 7(c) show images of the electrode and the circuit schematic respectively. The overall PCB height is 3.3cm, and again the same Default 8

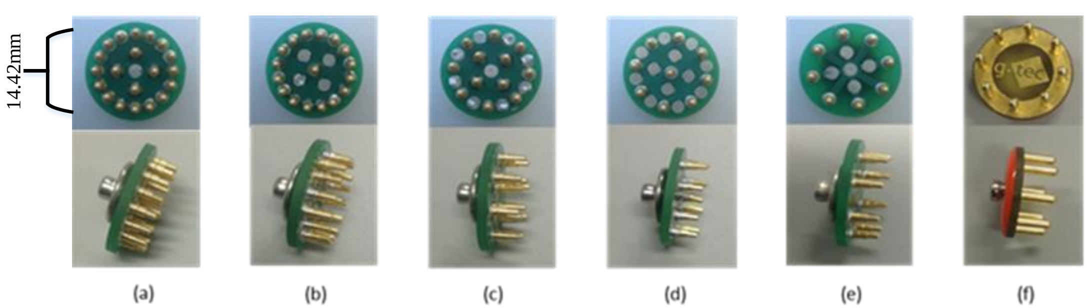

Figure 4 – (a) Circle 20: Outer ring of 16 fingers and an inner ring of 4 fingers (b) Circle 17: Outer ring of 16 fingers and one finger at center (c) Spread12: Outer ring of 8 fingers and an inner ring of 4 fingers (d) Center 9: Outer ring of 8 fingers and one finger at center (e) Default 8: Outer ring of 8 fingers (f) g.Sahara: Dry electrode by g.tec[14] (Image taken from [7])

configuration is used. As opposed to the IFC electrode which was built purely for experimental study, this MUX electrode can be considered a prototype to show the functionality of finger selection added to a typical electrode design.

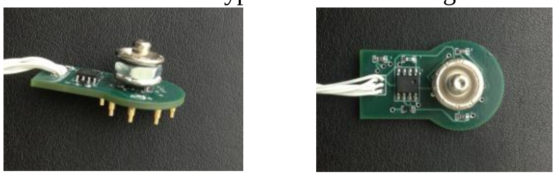

Figure 6 – MUX Electrode front and back (Image taken from [10])

E. Wet Electrode

We used the commercial Arbo pre-gelled ECG electrode as the reference electrode in all experiments in this work.

V. METHODS

Our working assumption throughout this study was that the impedance of contact of the dry electrode finger on the scalp is directly proportional to the amount of noise induced on the acquired signal. Most noise sources at the scalp electrode interface, such as the half-cell effect, have been shown to be directly proportional to the impedance of contact by previous studies [9]. Moreover, if the contact with the scalp is disrupted by hair, this would result in a high impedance contact and poor pickup of EEG. Hence, in this Section V, subsections A and B describe two different methods to estimate the impedance of contact. These were used in the study evaluating the relative merits of using different numbers of fingers in the electrode design. These techniques were then leveraged in the subsequent study looking into individual finger analysis and the possibility of improving the signal through finger selection as detailed in subsections C and D.

A. Impedance Excitation Response

To estimate scalp electrode impedance we can inject current at the signal electrode, shown as I_a in Figure 3. When this current is a sinusoid of known frequency f_0, then the frequency response of V_{out} at f_0 is dominated by the voltage drop across the overall impedance of the circuit due to the injected I_a. The power spectral peak of V_{out} at f_0 is termed the 'impedance excitation response', and is directly proportional to the impedance faced by the constant current I_a.

B. Common Mode Signal Injection

Another indirect measure of the scalp electrode contact impedance is the common mode rejection ratio (CMRR) of the circuit described in Figure 3. CMRR is a measure of how well the differential amplifier can reject signals that are common to both V_{sig} and V_{ref}. The output of the differential amplifier can be written as:

$$V_{out} = G_{diff}(V_{sig} - V_{ref}) + G_{cm}\frac{(V_{sig} + V_{ref})}{2} \qquad (4)$$

Where G_{diff} and G_{cm} represent the differential gain and common mode gain of the amplifier, respectively. EEG signals of interest are in the *difference* between the two measured signals given by the first term $G_{diff}(V_{sig} - V_{ref})$, and the common mode between the two electrodes is given by the second term and this is typically comprised of uniformly received sources of noise or other undesirable signals.

In ideal situations this common mode is rejected by the amplifier since G_{cm} is very small. In the ADS1299 analog front end used in this work for example, the ratio of G_{diff} to G_{cm} is at least 110dB [15]. However, CMRR decreases when there is an impedance mismatch between the two electrodes. For example, we consider the measurement of steady state visually evoked potentials (SSVEP), the brain's response to being presented with a visual stimulus at a regular frequency. These potentials are strongest at the occipital region at the back of the head [16] and so the signal electrodes are placed here while the reference electrode is placed in a region with suitably lower magnitude of SSVEP such as the right mastoid. EEG signals appearing elsewhere on the scalp, in the frontal region for example, as well as muscle artifacts are assumed to be picked up equally by both the signal and reference electrodes and become a part of the common mode. If the signal electrode faces a different impedance than the reference electrode, then it measures the 'common' signals differently

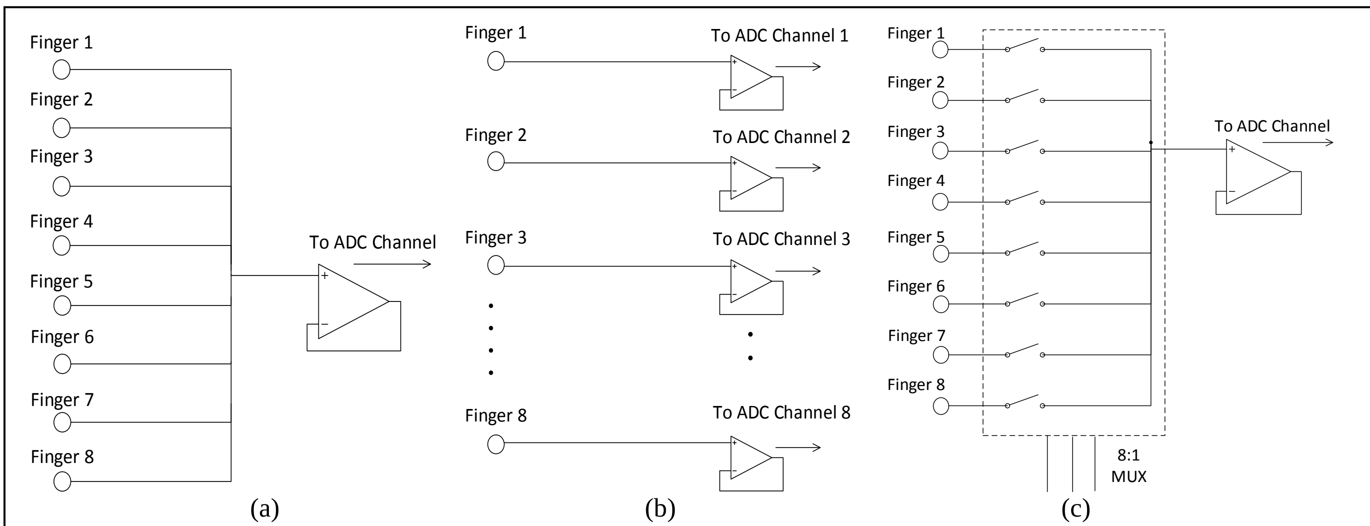

Figure 7 – (a) Traditional finger electrode circuit (b) IFC electrode circuit (c) MUX electrode circuit (Image taken from [10])

too. This in turn means that the frontal signals and the artifacts are no longer part of the common mode and become part of the differential mode instead. Thus, in the differential signals measured, the frontal signals and artifacts will be mixed in with the desired occipital signals.

In our experiments, one of the two electrodes is always a wet electrode with 'ideal' skin contact. This means that the relatively poor contact of the dry signal electrode results in an impedance mismatch with the reference electrode which in turn causes an increase of the common mode at the final output. In other words, as the contact impedance of the dry electrode gets better, and matches that of the ideal wet contact reference, the CMRR of the circuit improves. In practice, it is not easy to measure CMRR as the common noise entering the circuit at any given time is not easily characterized. However, a signal with known characteristics intentionally added to the common mode can serve as a common mode measurement trace. The CMRR can then be readily estimated by measuring the amount of rejection of this known signal at the output.

For bio-potential measurements, apart from the signal and reference electrodes, a third bias electrode is also attached to the body as part of an active driven right leg (DRL). This bias is applied equally to both the electrodes and hence is also a part of the common mode. In our design, shown in Figure 3, we add an AC square wave at a known frequency on top of this DC bias which will serve as the CMRR measurement trace. Any mismatch in contact impedance between electrodes would result in an increased presence of the square wave signal in the output. The power of the known common mode square wave frequency in V_{out} is thus directly proportional to the impedance faced by the signal electrode. This method of contact impedance estimation was previously shown in [8].

C. Exhaustive IFC Electrode Combination Analysis

Since the IFC electrode acquired signals from each individual finger independently and simultaneously, it afforded us the opportunity to uniformly compare the performances of all possible combinations of fingers for the same epoch of EEG. Exhaustively looking at all possible combinations is acceptable in this case since this electrode is meant only for experimental analysis offline and we wanted to ensure we could study the characteristics of the true optimum combination of fingers.

In our experiments, a wet electrode was placed right next to the IFC electrode to provide a ground truth signal. The noise on the wet electrode was assumed to be negligible and it is considered an ideal electrode. This is not strictly true since any electrode will be subject to some amount of noise, but we can safely assume that the amount of noise on the wet electrode is much lower than that on dry contacts and it is the best baseline available for EEG. Therefore, for each set of signals we have:

$$NoiseRMS_i = FingerRMS_i - WetRMS \tag{5}$$

Where i indicates a given finger on the electrode, $FingerRMS_i$ is the root mean square (RMS) of the signals from Finger i, $WetRMS$ is RMS of corresponding signals from wet electrode and $NoiseRMS_i$ is the RMS noise magnitude for Finger i. In the traditional finger electrode, we can model the finger contacts as impedances connected in parallel. Using the contact quality measure, we can obtain the impedance Z_i, and consequently the admittance Y_i, for each finger. Then for any given combination of fingers, we can calculate the contribution of each finger to the resulting parallel circuit. For example, for Fingers 1, 2 and 3 in parallel, the contribution fraction of Finger 1 is given by:

$$C_1 = \frac{Z_2 \parallel Z_3}{Z_1 + (Z_2 \parallel Z_3)} = \frac{Y_1}{Y_1 + Y_2 + Y_3} \tag{6}$$

In truth, the impedance is composed of both a resistance and capacitance so it would be frequency dependent; but we are only interested in the low frequency region where the electrode-skin interface noise, which is 1/f in nature, would dominate. Therefore, we can ignore the effect of the capacitance. Once we have the contribution fractions of each finger in a given combination, we can compute the overall RMS noise power for that finger combination as:

$$\sqrt{(C_1 \times NoiseRMS_1)^2 + \cdots + (C_n \times NoiseRMS_n)^2} \tag{7}$$

Where C_n is the contribution of finger n in the current combination and $NoiseRMS_n$ is the RMS noise magnitude of individual finger n defined earlier.

Similarly, we can also estimate the overall EEG signal, as opposed to just the noise, by applying the same contribution fraction on the signals from any combination of fingers:

$$Signal_x = C_1 \times Finger_1 + \cdots + C_n \times Finger_n \tag{8}$$

Where $Signal_x$ is the mixed EEG signal for finger combination x, C_n is the contribution of finger n in the current combination and $Finger_n$ is the EEG signal from Finger n.

D. MUX Electrode Finger Selection

A key difference between the IFC electrode and the MUX electrode is that different combinations of the MUX electrode fingers cannot be uniformly compared to each other due to the time delay involved in switching between the different combinations. This is an issue because the EEG signals they are measuring as well as the noise levels are non-stationary. So an exhaustive comparison of all possible finger combinations is not feasible. However, we found through IFC electrode experimental results, to be shown in Sections VII D and E, that individual fingers that exhibit poor impedance contact are likely to be noisier as well. Therefore, at the start of every MUX electrode experiment we heuristically identified a few good and bad fingers, based on the contact quality measure, and defined combinations that avoided the bad fingers. This process is further detailed in the experimental protocol of Section VI E.

VI. Experimental Setup

In this section we describe the objectives of the various experiments as well as the protocols. Subsection A aims to compare the different electrode types using impedance measurements on the scalp. Subsection B compares those same electrode types with the performance in a BCI task as the criteria. Subsection C repeats the impedance measurements of the electrodes on the hairless forearm to contrast with the effects of hair on scalp. Finally, subsections D and E describe the experimental protocols for IFC and MUX electrodes, respectively.

A. Impedance Measurement on Scalp

We defined three different use cases:

- No Adjust: The EEG cap is put on and no efforts are made to adjust the contact of the electrode
- Adjust: After putting on the cap, the electrode is twisted and pushed downwards in an effort to penetrate through the hair and make good contact
- Headband: After making efforts to penetrate the electrode through hair, we add a tight headband on top of the electrode to provide an additional downward push for better contact.

The reasoning behind defining these three use cases was to determine whether certain electrode designs would exhibit more robustness in the face of varying capping scenarios. The EEG cap used was a commercial one which was a part of the g.SAHARA system by g.tec. An example of the setup for measurement at FT8 with and without the headband is shown in Figure 8.

Figure 8 – Impedance measurement at FT8 without headband (left) and with headband (right)

One trial of the experiment consisted of about 10 seconds of current injection, with the impedance excitation response collected for each of the 10-second trials under each of the three use cases defined above. Three such trials were conducted for each electrode type in both the temporal FT8 position and the frontal AFZ position according to the 10-20 electrode placement system [17]. The cap was taken off and the hair was readjusted between trials to randomize the contact each time. The impedance excitation response was collected on six human subjects, with varying amounts of hair across subjects. A 24nA sinusoidal AC current at a frequency of 30.5Hz was injected and the peak of the power spectral density (PSD) estimate at that frequency was taken as the impedance excitation response in units of mV^2/Hz. This in-band frequency is a constraint of the hardware being used; the current injection circuits are internal to the ADS1299 chip and the frequency of current injection is fixed to be in-band.

B. SSVEP SNR and CMRR Measurement

SSVEPs, introduced in Section V B, are a well-known EEG response used in BCI tasks. We wanted to see if certain electrode designs elicited better, *i.e.* higher SNR, SSVEPs on average due to better contact. One session consisted of 4 separate trials of 10 seconds each with the subject fixating on the target flashing LED (18Hz frequency). Three such sessions were collected for each electrode type, with the cap taken off and put back on between sessions to randomize the contact. The data was collected for seven subjects in the 'Headband' case for the best possible contact scenario. The signal electrode was placed at the occipital location OZ, referenced to a wet electrode at the right mastoid. Successfully captured SSVEPs would result in a peak in the PSD of the EEG data at the target frequency. For SSVEP, SNR was defined as the ratio of the target frequency PSD peak to the peaks in the nearby non-target frequencies. The common mode square wave of 6mV amplitude was added at 61Hz throughout the tests and the PSD peak at this frequency was noted as the common mode signal power measured in units of $\mu V^2/Hz$. Since the common mode injection is done by our own custom circuit, the frequency of the signal is controllable and is set to be out-of-band for measurements simultaneously with EEG.

C. Impedance Measurement on Forearm

One of the major reasons we predicted for some electrode designs performing better than others was the ability to avoid hair. In order to confirm this effect, we designed a control experiment by measuring the impedance excitation response for the various electrode types with the signal electrode on the forearm in an area with little to no hair for seven subjects.

D. IFC Electrode Experiments

Alpha rhythms are strong EEG waveforms with known characteristics observed when a subject closes his/her eyes [3]. In contrast to SSVEP, this EEG response can be recorded on almost all parts of the scalp. This allowed us to use a wet electrode as an ideal electrode placed on the forehead in a region with no hair. The IFC electrode is placed right next to the wet electrode in a region with hair. We can safely assume that the EEG alpha signal will be almost identical between the two electrodes at this distance [4], but at the same time the fingers on the IFC electrode will pick up varying amounts of noise due to high impedance contact. We intentionally did not place electrodes at location OZ like the previous SSVEP measurement setup because, as will be confirmed by the results of the impedance measurement experiments, high impedance contact with hair is one of the factors in the increase of noise in the electrode. So we wanted to place the wet electrode in a region without any hair to ensure a clean gold standard signal, and also keep the IFC electrode in a region with hair for a more realistic, noisy and uneven contact among the different individual fingers. Since we want the EEG signals from these two electrodes to be largely the same, placing them next to each other on the forehead in this way and relying on alpha measurements was the only feasible option. Data was collected from 5 subjects with two sessions per subject. Each session involved 20 trials of about 10 seconds of eyes-closed alpha, with the electrode randomly readjusted between sessions to generate a larger variety of contacts to support the data set.

E. MUX Electrode Experiments

The MUX electrode experiments were designed in a similar manner to the IFC electrode experiment: 5 subjects performed the alpha task with the MUX electrode placed on the forehead close to a wet electrode for comparison. At the start of every session, on the MUX electrode, one finger was switched on while the rest of them were disconnected in order to measure that finger's contact impedance. The process was repeated in turn for each finger until we had the contact impedance of every individual finger. We then heuristically identified 4 or 5 'good' fingers, *i.e.* those fingers that had a relatively low impedance of contact, among the 8 available and then identified three combinations for each subject that involved only some subset of these good fingers. The objective was to see if any of these 'good combinations' performed better than the default case of using all eight fingers. So the experiment involved alternating between one trial of alpha for the good combination and one trial with the 'all fingers' combination. There were 30 trials for each combination leading to a total of 90 trials for each subject. Over this relatively large number of trials, we assume the better combination of fingers would on average show better correlation with the nearby wet electrode.

VII. Discussion of Results

A. Scalp Impedance Measurement

Tables I and II show the average impedance excitation responses (defined in Section V-A) for the different electrode types at the FT8 and AFZ scalp locations respectively. The data is ordered according to the three use cases: 'No Adjust', 'Adjust' and 'Headband' defined in Section VI-A. For both the scalp locations, the electrodes with lower density of fingers show better impedances in all use cases.

TABLE I: Average impedance excitation response at FT8

	Average Impedance Excitation Response (mV^2/Hz)		
Electrode Type	**No Adjust**	**Adjust**	**Headband**
Default 8	5,637.5	1,591.3	311.3
Center 9	8,663.5	1,923.1	287.0
Spread 12	8,895.9	2,102.5	174.8
Circle 17	21,617.3	7,679.6	470.3
Circle 20	46,327.5	19,853.5	1,029.4
g.SAHARA	9,037.6	3,059.8	511.4

TABLE II: Average impedance excitation response at AFZ

	Average Impedance Excitation Response (mV^2/Hz)		
Electrode Type	**No Adjust**	**Adjust**	**Headband**
Default 8	6,812.7	1,753.61	268.2
Center 9	9,822.0	831.4	67.9
Spread 12	6,046.5	738.9	38.3
Circle 17	28,294.4	4,420.1	692.5
Circle 20	68,994.5	8,026.9	376.0
g.SAHARA	10,157.2	3,864.9	150.8

When comparing the high density electrodes' (Circle 17 and Circle 20) impedance samples with those of the remaining low density electrodes (Default 8, Center 9, Spread 12 and g.SAHARA), the one-sided t-test showed a p-value < 0.004, thus rejecting the null hypothesis that the lower density electrodes show equal or higher impedance. This can be considered a statistically significant result since there are more than 100 samples of impedance for each electrode type when the data from all subjects and capping conditions is aggregated. It can also be observed that the higher density configurations show exceptionally high impedance excitation responses for the 'No Adjust' case and these responses are drastically reduced for the 'Headband' case. Repeating the above one-sided t-test for only the 'Headband' impedance data shows p-values as high as 0.22. This shows that these high density electrode types depend on effective preparation of scalp electrode contact by adjusting the electrode to penetrate through the hair, after which they could perform similarly to the low-density ones. Conversely, the low density configurations do not show as much variance between the 'No Adjust' and 'Headband' cases which indicates that they are more robust in the face of varying capping conditions.

B. SSVEP SNR and CMRR

Table III shows the average SSVEP SNR values (defined in Section VI-B) across all trials for seven subjects using the different electrode types as well as their respective common mode signal powers (defined in Section V-B).

TABLE III: Average SSVEP SNR and Common Mode Power

Electrode Type	Average SNR	Average Common Mode Signal Power ($\mu V^2/Hz$)
Default 8	4.097	1107.42
Center 9	4.035	818.28
Spread 12	3.927	2906.09
Circle 17	4.240	1637.51
Circle 20	3.781	4298.59
g.SAHARA	4.635	601.05

In most cases the SSVEP SNR of each electrode type is strongly correlated with its corresponding common mode signal power. As noted before, the SSVEP experiments were all conducted under ideal 'Headband' conditions, so the disparity in contact impedance between high and low density electrodes is not too large. The Circle 17 common mode power is suitably low due to this preparation, but the Circle 20 continues to have relatively poorer contact and this in turn adversely affects its SSVEP SNR. The data in general validates the assumption that EEG task performance is inextricably linked to the contact quality, and an electrode is unlikely to show a high performance with poor impedance contact. There was a negative correlation of -0.797 between average SNR of SSVEP and the corresponding common signal power. We also noted a significant performance difference between the Default 8 and g.SAHARA configurations despite their similar structure. The probable reason for this is the increased height and thickness of the fingers on the commercial g.SAHARA compared to our designs.

C. Forearm Impedance Measurement

Table IV shows the average impedance excitation response collected for each of the different electrode types as they were placed on the forearm of the seven subjects in an area with no hair. The results support the hypothesis that high density configurations suffer in performance primarily due to the effect of hair. Circle 17 and Circle 20 show a marked improvement in impedance compared to the other types.

TABLE IV: Average Impedance Excitation Response on forearm

Electrode Type	Average Impedance Excitation Response (mV^2/Hz)
Default 8	8285.49
Center 9	8502.23
Spread 12	7485.19
Circle 17	2777.65
Circle 20	3181.43

D. Individual Finger Analysis

In order to test the hypothesis that selecting a subset of fingers on a given electrode could improve the overall signal, we first attempted to show that the signals obtained from each individual finger could indeed be significantly different. We plotted the power spectrum of the signals from each of the fingers on the IFC electrode placed on the scalp as well as the signals from a wet electrode placed nearby for comparison. An illustrative case for one session of alpha on Human Subject 1 is shown in Figure 9. Only 7 fingers of the IFC electrode were used since the 8th channel of the EEG acquisition board was reserved for the clean signals from the wet electrode.

Evidently there are significant differences in the frequency spectrum, with at least four fingers – Fingers 2, 3, 4 and 5 – showing significantly higher noise levels compared to the others. The wet electrode has the least amount of noise and hence the lowest power as well. The peak at approximately 10Hz corresponds to the EEG response in the state of alpha. Among the three 'good' fingers - Fingers 6, 7 and 8 - the frequency response is mostly overlapped with that of the wet electrode in the higher frequencies, but there is a noticeable separation in the lower frequencies. This confirms that the noise experienced by the dry electrode fingers is 1/f in nature, which agrees with previous findings on skin interface noise [9]. Another observation is that the fingers with higher noise also showed worse contact quality. The example in Figure 9 shows in the upper right corner the corresponding rankings for the contact quality of the fingers according to the common mode based impedance measure described in Section V B. This confirms that the noise is related to the impedance of the contact and allowed us to use the common mode based contact quality measure as the basis for finger selection.

E. IFC Electrode Experiments

On the IFC electrode, the mixed signals from all possible combinations of fingers were exhaustively generated using the techniques described in Section V-C. The Noise RMS for each of these combinations of fingers was generated using Equation (7). For all subjects and sessions, there were always several combinations better than the 'all fingers' combination in terms of noise. The top four combinations in terms of noise magnitude as well as the combination corresponding to all fingers, averaged across all sessions and subjects are shown in Table V. Note that 'Best Combination #1' refers to the averaged noise magnitude from the very best combination from each session, but the identity and number of fingers that correspond to the best combination varies for different subjects and sessions due to the varying contact of the electrode.

TABLE V: Average RMS Noise magnitude for best finger combinations compared with 'all fingers' combination

Finger Combinations	Average RMS Noise magnitude (μV)
Best Combination #1	2.160
Best Combination #2	2.180
Best Combination #3	2.225
Best Combination #4	2.246
All Fingers	3.635

When comparing the averaged best combination on each subject to the corresponding RMS noise on the 'all fingers' case, the improvement is about 1.5μV. To put this in context, we can assume the wet electrode signal to be ideal and hence the average RMS of this, 13.91μV, estimates the magnitude of the true EEG signal. This means that in our experiments, the noise from the 'all finger' configuration constitutes 26% of the EEG signal, and using the best combination of fingers reduces this noise level by about 40% on average. This is also a statistically significant trend, as proved by the fact that a one-sided paired t-test between the noise from the best combination of fingers and the noise from the 'all fingers' case showed a p-value < 0.05 for 20 trials, thus invalidating the null hypothesis

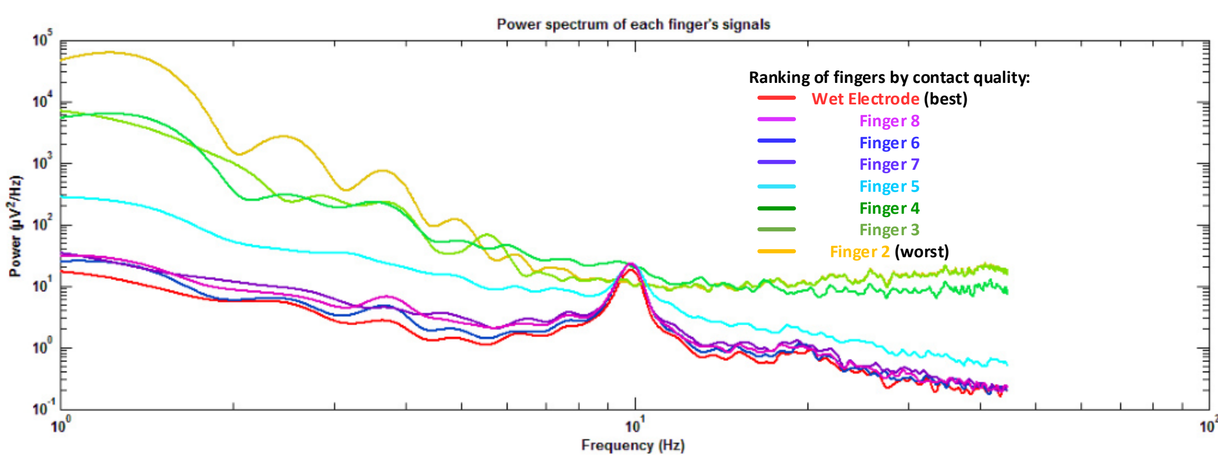

Figure 9 – Log scale plot of power spectrum from each of the fingers of IFC electrode and wet electrode (Image taken from [10])

that choosing fewer fingers does not reduce the noise.

We also generated the overall signal from each of the combinations as described by Equation (8). Signals from finger combinations with lower noise are expected to correlate better with the clean wet signal in the time domain. Again, for every session of data there were a few combinations of fingers that showed better correlation than the 'all fingers' case. The averaged correlation coefficients for the best four combinations of fingers, as well as the combination with all fingers, across all subjects and sessions are shown in Table VI. On average, the improvement in correlation with the wet electrode for each session was about 12.6% when using the best subset of fingers.

TABLE VI: Average correlation coefficient with wet electrode for best finger combinations compared with 'all fingers' combination

Finger Combinations	Average Cross Correlation Coefficient
Best Combination #1	0.815
Best Combination #2	0.812
Best Combination #3	0.808
Best Combination #4	0.808
All Fingers	0.724

F. *MUX Electrode Experiments*

With the MUX electrode, we can directly obtain signals from different combinations of fingers without the need for mixing based on electrode impedances. For each of the five subjects, at least one of the attempted combinations with fewer fingers showed better performance in terms of average correlation with the wet electrode, as shown in Table VII. These were also statistically significant performance improvements over the 15 trials of each session, with p-values < 0.05 in one-sided paired t-tests with the correlation coefficients of the nearest 'all fingers' trials for 4 of the 5 subjects studied. The corresponding p-value for Subject 4 was 0.1 and a possible reason for this was that the correlations with the wet electrode for this subject were relatively low for all trials and combinations.

TABLE VII: Performance comparison between selected MUX combinations vs the 'all fingers' combination for all five subjects

Subject	Average Correlation Coefficient (custom finger combination)	Average Correlation Coefficient (all 8 fingers selected)	p-value from one-sided paired t-test
Subject 1 Combo 1	0.903 (4 out of 8 fingers)	0.877 (all 8 fingers)	0.0297
Subject 2 Combo 1	0.951 (3 out of 8 fingers)	0.935 (all 8 fingers)	0.0086
Subject 2 Combo 2	0.962 (4 out of 8 fingers)	0.939 (all 8 fingers)	0.0151
Subject 3 Combo 1	0.912 (2 out of 8 fingers)	0.882 (all 8 fingers)	0.0425
Subject 4 Combo 2	0.699 (3 out of 8 fingers)	0.662 (all 8 fingers)	0.1258
Subject 5 Combo 1	0.746 (2 out of 8 fingers)	0.687 (all 8 fingers)	0.0458

However it must be noted that these combinations were found somewhat heuristically. In order to more extensively validate performance improvement on the MUX electrode we need to first overcome two challenges. Firstly, there is no a priori guarantee that the combination being selected for comparison is actually better than the 'all fingers' scenario. In other words, we are only looking at the contact qualities of the individual fingers relative to each other. There is no evidence yet to suggest a hard limit on the impedance measure, above which a finger must be considered to have a 'bad contact' and be excluded from any good combination. In fact, even during the MUX electrode experiments of this work, it might well be the case that none of the 'good' combinations we tried were the actual true optimum combination. Exhaustively trying all possible combinations in each new session is not an option; however a machine learning approach that trains over an extensive data set of different combinations of fingers and contact qualities may be a more feasible approach to predict a good combination. The second challenge is that the strength of the alpha response on a given subject may fluctuate during the course of one experiment. So the noise level of two different configurations cannot be compared uniformly if the desired signal level itself is changing dynamically. Apart from these two immediate challenges, one long term practical challenge is for the system to be adaptable to motion artifacts. A long term wearable solution would involve the electrode contacts varying frequently as the user moves around and the reconfigurable system must be ready for this. Overcoming these challenges and developing a real-time automatically reconfiguring MUX electrode will constitute our future work.

VIII. Conclusion

In this article, we described a methodology to uniformly compare different designs of finger-based dry electrodes to each other and demonstrated with experimental results that designs with a sparser arrangement of fingers were able to penetrate through hair better and were more robust to varying use cases. We also showed that individual fingers on an electrode can each have vastly differing signals due to differing contact impedances, and in turn, the ones with a bad contact could be picking up more local noise effects. We designed two custom electrodes to come to these conclusions and showed through experimental results that the overall signal from a given electrode can be improved by selecting only a subset of fingers with a good contact on the scalp.

Acknowledgment

This work was supported in part by the Semiconductor Research Corporation, task # 1836.103 through the Texas Analog Center of Excellence (TxACE). Any opinions, findings, conclusions, or recommendations expressed in this material are those of the authors and do not necessarily reflect the views of the funding organizations.

References

[1] E. W. Sellers, T. M. Vaughan, and J. R. Wolpaw, "A brain-computer interface for long-term independent home use," *Amyotrophic Lateral Sclerosis*, vol. 11, no. 5, pp. 449–455, 2010. PMID: 20583947.

[2] Y. Chi, T.-P. Jung, and G. Cauwenberghs, "Dry-contact and noncontact biopotential electrodes: Methodological review," *Biomedical Engineering, IEEE Reviews in*, vol. 3, pp. 106–119, 2010.

[3] T. Sullivan, S. Deiss, T.-P. Jung, and G. Cauwenberghs, "A brain-machine interface using dry-contact, low-noise eeg sensors," in *Circuits and Systems,*

2008. ISCAS 2008. IEEE International Symposium on, pp. 1986–1989, May 2008.

[4] R. Matthews, N. J. McDonald, H. Anumula, J. Woodward, P. J. Turner, M. A. Steindorf, K. Chang, and J. M. Pendleton, "Novel hybrid bioelectrodes for ambulatory zero-prep eeg measurements using multi-channel wireless eeg system," in *Proceedings of the 3rd International Conference on Foundations of Augmented Cognition*, FAC'07, (Berlin, Heidelberg), pp. 137–146, Springer-Verlag, 2007.

[5] L.-D. Liao, I.-J. Wang, S.-F. Chen, J.-Y. Chang, and C.-T. Lin, "Design, fabrication and experimental validation of a novel dry-contact sensor for measuring electroencephalography signals without skin preparation," *Sensors*, vol. 11, no. 6, pp. 5819–5834, 2011.

[6] Y. Chi, Y.-T. Wang, Y. Wang, C. Maier, T.-P. Jung, and G. Cauwenberghs, "Dry and noncontact eeg sensors for mobile brain #x2013;computer interfaces," *Neural Systems and Rehabilitation Engineering, IEEE Transactions on*, vol. 20, pp. 228–235, March 2012.

[7] V. Nathan and R. Jafari, "Characterizing contact impedance, signal quality and robustness as a function of the cardinality and arrangement of fingers on dry contact eeg electrodes," in *Engineering in Medicine and Biology Society (EMBC), 2014 36th Annual International Conference of the IEEE*, pp. 3755–3758, Aug 2014.

[8] T. Degen and H. Jackel, "Continuous monitoring of electrode–skin impedance mismatch during bioelectric recordings," *Biomedical Engineering, IEEE Transactions on*, vol. 55, pp. 1711–1715, June 2008.

[9] E. Huigen, "Noise in biopotential recording using surface electrodes," Master's thesis, University of Amsterdam, 2000.

[10] V. Nathan and R. Jafari, "Reducing the noise level of eeg signal acquisition through reconfiguration of dry contact electrodes," in *Biomedical Circuits and Systems Conference (BioCAS), 2014 IEEE*, pp. 572–575, Oct 2014.

[11] M. Reagor, C. Zong, and R. Jafari, "Maximizing information transfer rates in an ssvep-based bci using individualized bayesian probability measures," in *Engineering in Medicine and Biology Society (EMBC), 2014 36th Annual International Conference of the IEEE*, pp. 654–657, Aug 2014.

[12] O. Dehzangi, V. Nathan, C. Zong, C. Lee, I. Kim, and R. Jafari, "A novel stimulation for multi-class ssvep-based brain-computer interface using patterns of time-varying frequencies," in *Engineering in Medicine and Biology Society (EMBC), 2014 36th Annual International Conference of the IEEE*, pp. 118–121, Aug 2014.

[13] O. Dehzangi, Y. Zou, and R. Jafari, "Simultaneous classification of motor imagery and ssvep eeg signals," in *Neural Engineering (NER), 2013 6th International IEEE/EMBS Conference on*, pp. 1303–1306, Nov 2013.

[14] G. Edlinger, G. Krausz, and C. Guger, "A dry electrode concept for smr, p300 and ssvep based bcis," in *Complex Medical Engineering (CME), 2012 ICME International Conference on*, pp. 186–190, July 2012.

[15] Texas Instruments, *Low-Noise, 8-Channel, 24-Bit Analog Front-End for Biopotential Measurements*, 2012.

[16] G. Burkitt, R. Silberstein, P. Cadusch, and A. Wood, "Steady-state visual evoked potentials and travelling waves," *Clin. Neurophysiol.*, vol. 111, no. 2, pp. 246–258, 2000.

[17] H. H. Jasper, "Report of the committee on methods of clinical examination in electroencephalography: 1957," *Clin. Neurophysiol.*, vol. 10, pp. 370–375, 1958.

Viswam Nathan received his B.S. and M.S. degrees in computer engineering from the University of Texas at Dallas in 2012 and 2015 respectively.

He is currently working toward his Ph.D. degree in computer engineering at Texas A&M University. His research interests include design and development of a wearable and reconfigurable health monitoring devices as well as signal processing techniques to assess the quality and reliability of the acquired signal.

Roozbeh Jafari (SM'12) is an associate professor in Biomedical Engineering, Computer Science and Engineering and Electrical and Computer Engineering at Texas A&M University. He received his PhD in Computer Science from UCLA and completed a postdoctoral fellowship at UC-Berkeley. His research interest lies in the area of wearable computer design and signal processing. His research has been funded by the NSF, NIH, DoD (TATRC), AFRL, AFOSR, DARPA, SRC and industry (Texas Instruments, Tektronix, Samsung & Telecom Italia). He has published over 100 papers in refereed journals and conferences. He has served as the general chair and technical program committee chair for several flagship conferences in the area of Wearable Computers including the ACM Wireless Health 2012 and 2013, International Conference on Body Sensor Networks 2011 and International Conference on Body Area Networks 2011. He is the recipient of the NSF CAREER award in 2012, IEEE Real-Time & Embedded Technology & Applications Symposium (RTAS) best paper award in 2011 and Andrew P. Sage best transactions paper award from IEEE Systems, Man and Cybernetics Society in 2014. He is an associate editor for the IEEE Sensors Journal, IEEE Internet of Things Journal and IEEE Journal of Biomedical and Health Informatics.